Original Article

Use of diffusion-weighted magnetic resonance imaging (DW-MRI) to predict early response to anti-tumor therapy in advanced non-small cell lung cancer (NSCLC): a comparison of intravoxel incoherent motion-derived parameters and apparent diffusion coefficient

Zheng Yuan[1#], Xiao-Min Niu[2#], Xue-Mei Liu[3], Hong-Chao Fu[3], Ting-Jia Xue[3], Chi Wan Koo[4], Katsuhiro Okuda[5], Feng Yao[6], Xiao-Dan Ye[3,7]

[1]Department of Radiology, Huadong Hospital, Fudan University, Shanghai, China; [2]Department of Medical Oncology, Shanghai Chest Hospital, Shanghai Jiao Tong University, Shanghai, China; [3]Department of Radiology, Shanghai Chest Hospital, Shanghai Jiao Tong University, Shanghai, China; [4]Department of Radiology, Mayo Clinic, Rochester, Minnesota, USA; [5]Department of Oncology, Immunology and Surgery, Nagoya City University Graduate School of Medical Sciences, Nagoya, Japan; [6]Department of Thoracic Surgery, Shanghai Chest Hospital, Shanghai Jiao Tong University, Shanghai, China; [7]Department of Radiology, Zhongshan Hospital, Fudan University, Shanghai, China

Contributions: (I) Conception and design: F Yao, XD Ye; (II) Administrative support: XM Liu, HC Fu; (III) Provision of study materials or patients: XM Niu, F Yao; (IV) Collection and assembly of data: Z Yuan, XD Ye; (V) Data analysis and interpretation: Z Yuan, XM Niu, XD Ye; (VI) Manuscript writing: All authors; (VII) Final approval of manuscript: All authors.

[#]These authors contributed equally to this work.

Correspondence to: Dr. Feng Yao. Department of Thoracic Surgery, Shanghai Chest Hospital, Shanghai Jiao Tong University, 241 West Huai Hai Road, Shanghai 200050, China. Email: yaofeng6796678@126.com; Dr. Xiao-Dan Ye. Department of Radiology, Shanghai Chest Hospital, Shanghai Jiao Tong University, 241 West Huai Hai Road, Shanghai 200050, China. Email: yuanyxd@163.com.

Background: The intravoxel incoherent motion (IVIM) method of magnetic resonance imaging (MRI) analysis can provide information regarding many physiological and pathological processes. This study aimed to investigate whether IVIM-derived parameters and the apparent diffusion coefficient (ADC) can act as imaging biomarkers for predicting non-small cell lung cancer (NSCLC) response to anti-tumor therapy and compare their performances.

Methods: This prospective study included 45 patients with NSCLC treated with chemotherapy (29 men and 16 women, mean age 57.9±9.7 years). Diffusion-weighted imaging was performed with 13 b-values before and 2–4 weeks after treatment. The IVIM parameter pseudo-diffusion coefficient (D*), perfusion fraction (f), diffusion coefficient (D), and ADC from a mono-exponential model were obtained. Responses 2 months after chemotherapy were assessed. The diagnostic performance was evaluated, and optimal cut-off values were determined by receiver operating characteristic (ROC) curve analysis, and the differences of progression-free survival (PFS) in groups of responders and non-responders were tested by Cox regression and Kaplan-Meier survival analyses.

Results: Of 45 patients, 30 (66.7%) were categorized as responders, and 15 as non-responders. Differences in the diffusion coefficient D and ADC between responders and non-responders were statistically significant (all $P<0.05$). Conversely, differences in f and D* between responders and non-responders were both not statistically significance (all $P>0.05$). The ROC analyses showed the change in D value (ΔD) was the best predictor of early response to anti-tumor therapy [area under the ROC curve (AUC), 0.764]. The Cox-regression model showed that all ADC and D parameters were independent predictors of PFS, with a range of reduction in risk from 56.2% to 82.7%, and ΔD criteria responders had the highest reduction (82.7%).

Conclusions: ADC and D derived from IVIM are potentially useful for the prediction of NSCLC treatment response to anti-tumor therapy. Although ΔD is best at predicting response to treatment, ΔADC

measurement may simplify manual efforts and reduce the workload.

Keywords: Intravoxel incoherent motion (IVIM); diffusion-weighted imaging (DWI); apparent diffusion coefficient (ADC); non-small cell lung cancer (NSCLC); response evaluation criteria

Submitted Jun 07, 2021. Accepted for publication Aug 18, 2021.
doi: 10.21037/tlcr-21-610
View this article at: https://dx.doi.org/10.21037/tlcr-21-610

Introduction

Over the past two decades, diffusion-weighted magnetic resonance (MR) imaging (DW-MRI) detecting tissue cellularity and extracellular matrix properties *in vivo* has been widely applied to distinguish malignant and benign tumors and evaluate tumor response to therapy (1,2). The intravoxel incoherent motion (IVIM) method of MRI analysis using the bi-exponential model further separates diffusion images into pure diffusion and perfusion without contrast agent injection, and promising results that IVIM parameters can provide information regarding many physiological and pathological processes have been reported. IVIM parameters can be used as surrogate markers to identify benign and malignant tumors (3,4), distinguish lung cancer from inflammatory lesions (5), and improve the diagnostic performance of mediastinal lymph nodes compared to using apparent diffusion coefficient (ADC) alone (6). IVIM parameters from IVIM can be used to assess tumor proliferation by analyzing the correlations between the diffusion-weighted imaging (DWI)-derived parameters and Ki-67 expression (7). The perfusion-related parameters of IVIM DWI offer an alternative to dynamic contrast-enhanced (DCE)-MRI for evaluating tumor perfusion and serve as markers of the efficacy of tumor anti-vascular therapies without contrast media injection. The previous study had shown that a good correlation between IVIM parameters and DCE-MRI (Ktrans); and the relative change in IVIM parameters f and fD* at 2 hours correlated well with changes in tumor volume on day 8 (8).

DW-MRI and ADCs have been reported to be useful for the assessment lung cancer response to therapy. To our knowledge, there is no study to compare performances of bi-exponential model DW-MRI parameters and mono-exponential model DW-MRI parameter ADC in assessment non-small cell lung cancer (NSCLC) response to anti-tumor therapy. The present study aimed to investigate whether the parameters of pure diffusion coefficient (D), pseudo-diffusion coefficient (D*), and perfusion fraction (f) derived from IVIM DW-MRI could be used to evaluate early changes in tumor tissue perfusion and diffusion in patients with advanced NSCLC receiving anti-tumor therapy. Furthermore, we examined the performance of IVIM parameters against that of ADC in predicting the therapeutic responses of NSCLC tumors. We present the following article in accordance with the STARD reporting checklist (available at https://dx.doi.org/10.21037/tlcr-21-610).

Methods

Patients

All procedures performed in this study involving human participants were in accordance with the Declaration of Helsinki (as revised in 2013). The study was approved by ethics board of Shanghai Chest hospital, Shanghai Jiao Tong university (NO.: ks1832) and informed consent was taken from all the patients.

The inclusion criteria were (I) NSCLC patients with definite pathologic diagnosis and chemotherapy decisions; (II) the presence of a computed tomography (CT) detected measurable solid nodule or mass with the longest diameter greater than 1.0 cm. The exclusion criteria were (I) contraindications to MRI examination, and (II) patients whose DW-MRI quality did not allow for calculating DWI-related parameters due to excessive motion artifacts, severe magnetic susceptibility artifact, and other causes.

Baseline characteristics were recorded for each patient, including age, gender, smoking history, type of histopathology, and TNM stage before treatment.

MRI

All MRI was performed with a 1.5T (Achieva 1.5T, Philips Healthcare, Best, the Netherlands) or a 3.0T MR scanner (Ingenia 3.0T, Philips Healthcare, Best, the Netherlands) using a 16-channel Torso coil within 1 week before treatment and 2–4 weeks after the start of the first cycle of anti-tumor

therapy. Routine MR sequences included axial gradient echo T1-weighted (T1W) imaging [repetition time (TR)/ echo time (TE) 3.0/1.0 ms, flip angle 100, section thickness/ gap 6.0/0.6 mm], and axial and coronal turbo spin-echo T2-weighted (T2W) imaging (TR/TE 3,335.0/80.0 ms, flip angle 900, section thickness/gap 4.0/1.0 mm). The MR images were obtained during end-inspiration breath-holding.

DWI with thirteen b values (0, 5, 10, 15, 20, 25, 50, 80, 100, 200, 400, 600, and 800) was performed by using a single-shot, spin-echo, echo-planar imaging sequence in the transverse plane with free breathing. The slice locations of the DWI sequence were copied from the T2-weighted images to facilitate anatomic reference, and the parameters were a TR/TE of 1,674 ms/64 ms, a slice thickness of 4.0 mm with a gap of 1.0 mm, and a field of view of 375*300 mm^2. Parallel imaging was used with an acceleration factor of 3 and a half-scan factor of 69.8%. The receiver bandwidth was 3,475.5 Hz/pixel, and fat was suppressed using spectral pre-saturation inversion recovery (SPIR). The total acquisition time was 3 min 16 s.

Image analysis

Quantitative analysis of all MR images was performed on a dedicated post-processing workstation (MR Body Diffusion Toolbox, syngo. via Frontier, Siemens, Erlangen, Germany).

Regions of interest (ROIs) were drawn to encompass as much of the homogeneous area of the lesion as possible on the image of the largest cross-sectional tumor area by reference to conventional MR images. All ROIs were placed in consensus by two radiologists (XD Ye and Z Yuan, with 14 and 16 years of experience in MRI diagnosis, respectively), and the mean value of the two measurements was obtained. Monoexponential ADC was calculated by using b_{min} 50 s/mm^2 and b_{max} 800 s/mm^2. The change in ADC, D, f, and D* values (ΔADC, ΔD, Δf, and ΔD*) after treatment was calculated as follows:

$$\Delta(ADC/D/f/D^*) = (ADC/D/f/D^*)_{post} - (ADC/D/f/D^*)_{pre} \quad [1]$$

where *post* means after treatment, *pre* means before treatment, D is the true diffusion coefficient, D* is the pseudo-diffusion coefficient, and f is the perfusion fraction.

The percent of ADC, D, f, and D* changing values (%ΔADC, %ΔD, %Δf, and %ΔD*) after treatment was calculated as follows:

$$\%\Delta(ADC/D/f/D^*) = [(ADC/D/f/D^*)_{post} - (ADC/D/f/D^*)_{pre}]/(ADC/D/F/D^*)_{pre} \times 100\% \quad [2]$$

When there were multiple measurable lung lesions, the MRI parameter measurement was performed for one dominant lesion.

Tumor radiologic response assessment by Response Evaluation Criteria in Solid Tumors (version 1.1) (RECIST 1.1)

Radiologic interpretation according to revised RECIST 1.1 (9) was provided by two radiologists (XD Ye and Z Yuan) according to pre-treatment (performed within 1 week prior to the first cycle of anti-tumor therapy) and post-treatment CT studies (performed 8 weeks after the start of the first course of anti-tumor therapy) on picture archiving and communication systems workstations. Review sessions were carried out independently and on different days. In the case of a discrepancy in response assessment, the images were reviewed together by the radiologists and a consensus decision was reached.

Patients were followed-up by medical and oncology services every month until disease progression, and imaging assessment was performed at 1-month intervals.

Statistical analysis

All numeric data were presented as mean ± standard deviation (SD). Independent sample *t*-tests were used to detect significant differences for the data with a normal distribution evaluated by the Kolmogorov-Smirnov test, and for data without the assumption of a normal distribution, the non-parametric Mann-Whitney U test was used.

Receiver operating characteristic (ROC) curve analysis was used to evaluate the DW-MRI parameters performance in predicting early response to treatment and to determine the optimal cut-off value, which was defined as the point that yielded the best sensitivity and specificity based on the Youden Index for evaluating response to treatment.

For the calculation of progression-free survival (PFS), disease progression defined by RECIST 1.1 or death was used as an endpoint. The PFS time interval was defined as the time between the day of initial treatment and the date of imaging study just before the imaging study identified disease progression or death. By the time of analysis (July 2018), all patients showed disease progression. Cox regression and Kaplan-Meier survival analyses were used to explore the differences in PFS between the responders and non-responders according to RECIST 1.1, the IVIM parameters, and the ADC criteria. The Cox proportional

Table 1 Patient baseline characteristics and univariate analysis of the association between PFS and clinical characteristics

Demographics	Values	PFS	
		HR (95% CI)	P value
Total number of patients	45		
Age at diagnosis (years), mean (SD)	57.9 (9.7)	1.003 (0.972, 1.035)	0.849
Gender, n (%)			
Male	29 (64.4)	1.000	0.773
Female	16 (35.6)	0.912 (0.489, 1.701)	
Smoking history, n (%)			
Yes	19 (42.2)	1.000	0.410
No	26 (57.8)	0.775 (0.422, 1.422)	
Histopathological type, n (%)			
Adenocarcinoma	28 (62.2)	1.000	0.016
Squamous cell carcinoma	17 (37.8)	2.274 (1.163, 4.446)	
T staging, n (%)			
1	7 (15.6)	1.000	0.222
2	21 (46.7)	0.831 (0.295, 2.341)	
3	8 (17.8)	0.506 (0.224, 1.144)	
4	9 (20)	1.042 (0.399, 2.723)	
N staging, n (%)			
x	2 (4.4)		
0	4 (8.9)	1.000	0.569
1	2 (4.4)	2.162 (0.722, 6.472)	
2	12 (26.7)	0.909 (0.270, 3.062)	
3	25 (55.6)	1.084 (0.527, 2.231)	
M staging, n (%)			
x	3 (6.7)		
0	11 (24.4)	1.000	0.706
1	31 (68.9)	0.874 (0.434, 1.759)	

PFS, progress-free survival; HR, hazard ratio; CI, confidence interval.

model was employed to estimate the hazard ratio (HR) of each category compared to the non-responders among each method, respectively.

Statistical significance was considered for P<0.05. SPSS software version 22.0 (IBM, Armonk, NY, USA) was used to perform the statistical analyses.

Results

Patient baseline characteristics

A total of 49 consecutive patients received chest MRI examinations. After reviewing the MR images, three patients were excluded because of insufficient image quality caused by motion, susceptibility artifacts (n=2), or lesions smaller than 1 cm on CT (n=1), and one was excluded because of a lack of a pathologic diagnosis. Thus, a total of 45 subjects (29 men and 16 women, mean age 57.9±9.7 years) were included. Most cases were adenocarcinomas (n=28), and the remainder were squamous cell carcinomas. The chemotherapy regimens used in this study were cisplatin and pemetrexed (n=18), cisplatin and gemcitabine (n=15), cisplatin and docetaxel (n=7), cisplatin and vinorelbine (n=3), and carboplatin and paclitaxel (n=2). Detailed patient characteristics are summarized in *Table 1*.

IVIM parameters and ADC values between responders and non-responders evaluated by RECIST 1.1

After treatment, all ADC, f, D, and D* values were higher than before treatment, although the differences were not all statistically significant (*t*-test, all P>0.05). Thirty (66.7%) of 45 patients were categorized as responders (all partial response), and 15 (33.3%) were non-responders (including 12 patients categorized as stable diseases and three patients as progressive diseases) evaluated by RECIST 1.1 (*Figure 1*). The ADC values and IVIM parameters of responders and non-responders are summarized in *Table 2*.

The responders had lower pre-treatment ADC values and larger changes in ADC values (ΔADC) and percent changes in ADC values (%ΔADC) after treatment than the non-responders, and these differences were statistically significant (all P<0.05). There were no statistically significant differences in the post-treatment ADC values between the responders and non-responders (P=0.324).

Similarly, the responders had higher post-treatment D values and larger changes in D values (ΔD) and percent changes in D values (%ΔD) after treatment than the non-responders, and these differences were statistically significant (all P<0.05).

The differences in f and D* values between the responders and non-responders were both not statistically significant (all P>0.05).

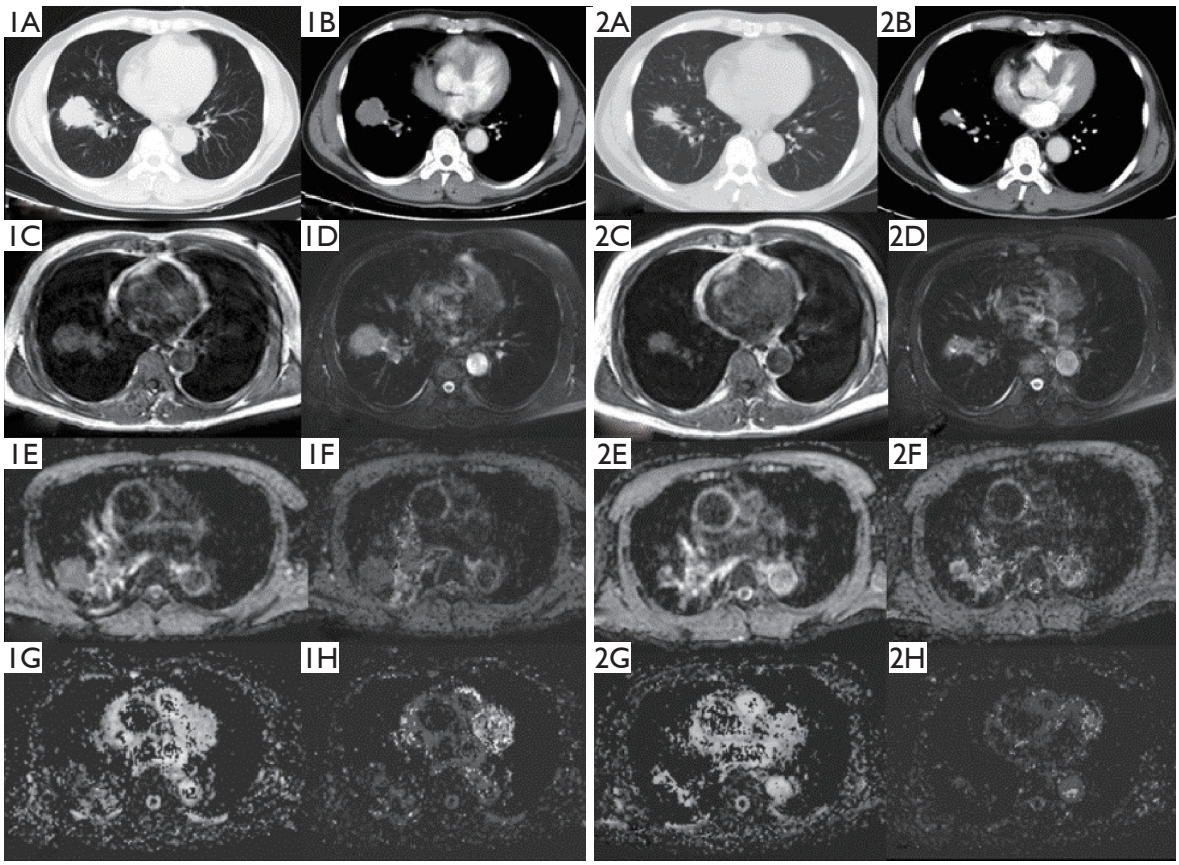

Figure 1 Representative example of transverse images in a 60-year-old man with lung cancer (adenocarcinoma, T2N3M1, stage IV) achieving partial response after two courses of chemotherapy evaluated by RECIST 1.1. (1A-1H) Pre-chemotherapy axial images; (2A-2H) post-chemotherapy axial images. (1A,1B,2A,2B) Before (1A,1B) and after (2A,2B) two courses of chemotherapy show a substantial interval change in size. (1C,2C) T1W imaging demonstrates a mass with intermediate signal intensity. (1D,2D) T2W imaging demonstrates high signal intensity. (1E-1H,2E-2H) Before (1E-1H) and 4 weeks after (2E-2H) chemotherapy parameter map of ADC, D, f, and D* calculated from DWI data. The measured ADC, D, f, and D* values before and 4 weeks after chemotherapy were 1.09×10^{-3} *vs.* 1.51×10^{-3} mm^2/s, 1.29×10^{-3} *vs.* 1.41×10^{-3} mm^2/s, 40.3% *vs.* 57.9% and 16.3×10^{-3} *vs.* 30.1×10^{-3} mm^2/s, respectively. RECIST 1.1, Response Evaluation Criteria in Solid Tumors (version 1.1); T1W, T1-weighted; T2W, T2-weighted; ADC, apparent diffusion coefficient; D, pure diffusion coefficient; D*, pseudo-diffusion coefficient; f, perfusion fraction.

Optimal cut-off values of IVIM parameters and ADC values to predict early response to treatment

To establish the functional imaging parameters' evaluation response to the therapy criteria, the ADC and D parameters that had statistically significant differences between the responders and non-responders were selected and ROC curve analyses were performed to evaluate their diagnostic performance in predicting early response to treatment and to determine the optimal cut-off values.

The results of the ROC analyses are summarized in *Table 3*. All pre-ADC, ΔADC, %ΔADC, post-D, ΔD, and %ΔD values could be used to predict early response to treatment, with areas under the ROC curve (AUCs) of 0.702 (95% CI: 0.535, 0.869), 0.731 (95% CI: 0.567, 0.896), 0.718 (95% CI: 0.554, 0.881), 0.754 (95% CI: 0.609, 0.900), 0.764 (95% CI: 0.590, 0.939), and 0.751 (95% CI: 0.572, 0.930), respectively. Using the optimal cut-off value of -0.294×10^{-3} mm^2/s, ΔD was shown to be the best predictor of early response to treatment (AUC 0.764).

Association with PFS

Kaplan-Meier methods were used to calculate the median

Table 2 IVIM parameters and ADC of advanced non-small cell lung cancer in early response to anti-tumor therapy evaluated by RECIST 1.1 criteria

Parameters	Responders	Non-responders	P value
ADC ($\times10^{-3}$ mm^2/s)			
Pre-	1.22 (0.2)	1.52 (0.51)	0.028[a]
Post-	1.48 (0.47)	1.35 (0.25)	0.324[b]
Δ	0.26 (0.53)	−0.17 (0.49)	0.011[b]
%Δ	25.2 (46.6)	−5.0 (29.9)	0.028[b]
D ($\times10^{-3}$ mm^2/s)			
Pre-	1.12 (0.24)	1.31 (0.45)	0.076[b]
Post-	1.33 (0.33)	1.09 (0.19)	0.013[b]
Δ	0.21 (0.41)	−0.22 (0.46)	0.003[b]
%Δ	24.3 (47.5)	−8.87 (33.8)	0.020[b]
f (%)			
Pre-	36.3 (8.6)	40.4 (14.6)	0.579[b]
Post-	41.4 (12.1)	41.8 (11.5)	0.919[b]
Δ	5.04 (12.2)	1.34 (14.1)	0.367[b]
%Δ	17.4 (35.0)	11.2 (38.9)	0.593[b]
D* ($\times10^{-3}$ mm^2/s)			
Pre-	20.4 (6.39)	22.3 (9.68)	0.772[a]
Post-	24.3 (8.98)	23.5 (5.52)	0.764[b]
Δ	3.89 (11.8)	1.23 (9.96)	0.458[b]
%Δ	29.9 (57.1)	20.9 (47.2)	0.598[b]

Data were means with ranges in parentheses. [a], Mann-Whitney U test; [b], *t*-test. RECIST 1.1, Response Evaluation Criteria in Solid Tumors (version 1.1); IVIM, intravoxel incoherent motion; ADC, apparent diffusion coefficient; D, pure diffusion coefficient; f, perfusion fraction; D*, pseudo-diffusion coefficient.

PFS of the responders and non-responders for each criterion (*Table 4* and *Figure 2*), and the differences in PFS between the responders and non-responders evaluated by each of the ADC and D parameters criteria (including pre-ADC, ΔADC, %ΔADC, post-D, ΔD, and %ΔD) were statistically significant (all P<0.05). For the ΔADC and ΔD criteria, the responders' median PFS were both 32 weeks and non-responders' median PFS were both 16 weeks (log-rank test, P=0.001 and P<0.001, respectively). Differences in PFS between responders and non-responders evaluated by RECIST 1.1 using CT were not statistically significant (31 *vs.* 21 weeks, log-rank test, P=0.107). Using the ADC and D parameters criteria are better than RECIST 1.1 using CT in evaluation PFS.

The association between each criterion and PFS was assessed using Cox regression and the statistical difference was determined (*Table 4*). The ΔADC responders had a 64.9% reduction in risk compared to non-responders, whereas the ΔD and %ΔD responders both had an 85.8% reduction in risk.

Finally, a univariate analysis confirmed the histopathological type as a significant prognosticator of PFS (*Table 1*). Using this factor, we applied backward selection to construct six multivariate models which examined the association of pre-ADC, ΔADC, %ΔADC, post-D, ΔD, and %ΔD responses with PFS, and all the models showed that pre-ADC, ΔADC, %ΔADC, post-D, ΔD, and %ΔD were significant risk factors. These functional imaging criteria derived from the diffusion-weighted MRI responders had a range of reduction in risk from 56.2% to 82.7%, with the ΔD and %ΔD criteria responders both having the highest reduction in risk at 82.7% compared to the non-responders. All these functional imaging

Table 3 Diagnostic performance of the cut-off values of using selected diffusion parameters for discriminating advanced non-small cell lung cancer response to anti-tumor therapy

Parameters	AUC (95% CI)	Cut-off	Sensitivity	Specificity	Youden Index
ADC					
Pre-ADC	0.702 (0.535, 0.869)	1.41×10^{-3} mm^2/s	90%	53.3%	0.433
ΔADC	0.731 (0.567, 0.896)	-0.049×10^{-3} mm^2/s	80%	66.7%	0.467
%ΔADC	0.718 (0.554, 0.881)	−1.40%	76.7%	73.3%	0.500
D					
Post-D	0.754 (0.609, 0.900)	1.13×10^{-3} mm^2/s	76.7%	60%	0.367
ΔD	0.764 (0.590, 0.939)	-0.294×10^{-3} mm^2/s	96.7%	60%	0.567
%ΔD	0.751 (0.572, 0.930)	−22.5%	96.7%	60%	0.567

ADC, apparent diffusion coefficient; D, pure diffusion coefficient; AUC, area under the curve; CI, confidence interval.

Table 4 Univariate Kaplan-Meier survival and Cox regression of responders and non-responders by the RECIST 1.1, ADC, and D criteria, respectively

Parameters	No. of patients (out of 45)	Median PFS (95% CI) (weeks)	P value by log-rank test	PFS HR (95% CI)	P value by Cox model
RECIST 1.1			0.107		0.123
Non-responders	15	21 (15.951, 26.049)		1.000	
Responders	30	31 (26.974, 35.026)		0.606 (0.320, 1.145)	
Pre-ADC			<0.001		0.003
Non-responders	12	16 (13.866, 18.134)		1.000	
Responders	33	32 (28.661, 35.339)		0.307 (0.151, 0.623)	
ΔADC			0.001		0.001
Non-responders	16	16 (14.102, 17.898)		1.000	
Responders	29	32 (29.363, 34.637)		0.351 (0.185, 0.668)	
%ΔADC			<0.001		<0.001
Non-responders	18	16 (14.378, 17.622)		1.000	
Responders	27	33 (28.929, 37.071)		0.321 (0.169, 0.606)	
Post-D			0.003		0.005
Non-responders	16	18 (10.160, 25.840)		1.000	
Responders	29	32 (29.363, 34.637)		0.394 (0.205, 0.755)	
ΔD			<0.001		<0.001
Non-responders	10	16 (12.964, 19.036)		1.000	
Responders	35	32 (28.534, 35.466)		0.142 (0.057, 0.356)	
%ΔD			<0.001		<0.001
Non-responders	10	16 (12.964, 19.036)		1.000	
Responders	35	32 (28.534, 35.466)		0.142 (0.057, 0.356)	

RECIST, Response Evaluation Criteria in Solid Tumors; ADC, apparent diffusion coefficient; D, pure diffusion coefficient; PFS, progress-free survival; HR, hazard ratio; CI, confidence interval.

criteria responses were independent risk factors for PFS.

Discussion

The accurate imaging evaluation of tumor response to therapy is important for determining the efficacy of therapy and subsequent therapeutic planning, and as surrogate markers for improved survival. Functional imaging is a potentially promising technique for the assessment of cancer response to therapy, and in this prospective study, the functional imaging parameters ADC and D derived from IVIM showed predictive utility for the early evaluation of NSCLC response to chemotherapy and were independent predictors of PFS.

We first compared the ADC and IVIM parameters between responders and non-responders as evaluated by RECIST 1.1 criteria after treatment. Optimal parameters were then selected, and a ROC curve analysis was used to evaluate their performance of predicting early response to treatment. Higher ΔADC, %ΔADC, ΔD, and %ΔD after treatment were all found in the responders than the non-responders, which confirmed previously reported associations between early ADC changes and eventual tumors responses to therapy (10-12). A larger increase in ADC after therapy was consistently associated with a more favorable outcome or with a higher degree of necrosis at histopathologic examination (13). Previous research also showed that the ADC value was significantly negatively

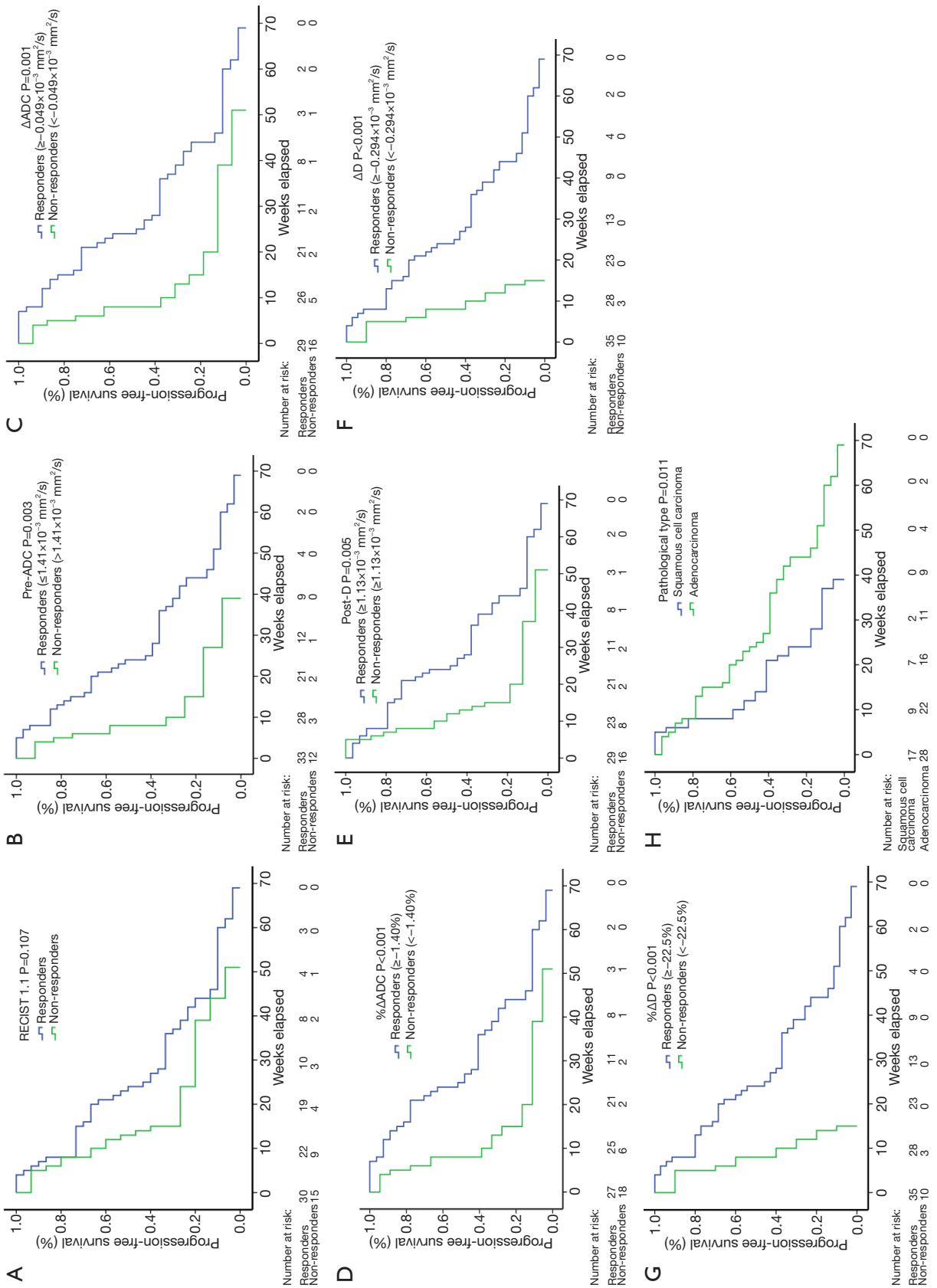

Figure 2 Kaplan-Meier curves show comparison of PFS between responders (complete and partial response, blue curve) and non-responders (stable and progressive disease, green curve) at 2-month imaging as assessed by means of RECIST 1.1 (A), pre-ADC (B), ΔADC (C), %ΔADC (D), post-D (E), ΔD (F), %ΔD (G), and pathological type (H). P values are shown in the figure. PFS, progression-free survival; RECIST 1.1, Response Evaluation Criteria in Solid Tumors (version 1.1); ADC, apparent diffusion coefficient; D, pure diffusion coefficient; ΔADC, changes in ADC values; ΔD, changes in D values; %ΔADC, percent changes in ADC values; %ΔD, percent changes in D values.

correlated with tumor cellularity in patients with lung cancer, and that tumor cellularity was most likely not the sole determinant of the ADC (14). As one of the IVIM parameters, D reflects the diffusion of water molecules in tissue dependent on cell density and components of the extracellular matrix. This means the D value decreased when tissue contained a high number of cells and ratio of nucleus to the cytoplasm, or with smaller extracellular space because of the diffusion movement of water molecule was limited (15). As shown in previous studies (7,16,17), tumor cell death by necrosis or apoptosis caused by anticancer drugs reduces cell density and increases the tumor extracellular volume in early response. Recent study showed D values from IVIM were negatively correlated with Ki-67 expression, which is likely that the highly proliferative tumors (high Ki-67 expression) had higher inner structural complexities due to increased cellularity, vascular hyperplasia, and necrosis (7), and this is the biological basis for the observed increase in ADC and D after treatment. Furthermore, because ADC is obtained from a mono-exponential model using diffusion-weighted MR imaging which is subject to errors introduced by the microcirculation of blood, D showed a higher performance at predicting response to therapy than ADC.

Although both D* and f are perfusion-related parameters in the IVIM sequence (15), they represent different characteristics of blood perfusion (18). D* mainly measures the average blood velocity, while f measures fractional blood volume in the capillary network, which reflects the microscopic translational motion associated with the microcirculation of blood. Previous studies have shown that the perfusion-related parameters D* and/or f can be used to predict the efficacy of anti-vascular therapies without the need for contrast media injection in tumor perfusion (8) and pulmonary antifungal treatment (19), and to differentiate lung cancer from inflammatory lung lesions (5). In this study, the D* and f values of NSCLC after chemotherapy were all slightly higher than before treatment, and the change in the values of D* and f in the responders was slightly larger than in the non-responders, but none of the differences were statistically significant. One possible reason for these different results may be that varying types of treatment may greatly affect the perfusion-related parameter results. In our study, the chemotherapy for NSCLC was cytotoxic therapy, which at early time points may not influence the state of tumor perfusion. At the same time, other factors, including the characteristics of tissues in the magnetic field, echo time, and relaxation time of the MRI scanning may also greatly affect the f value (20,21).

Overall survival (OS) and PFS are generally accepted as the major endpoints for clinical trials in tumor treatment, but radiological evaluation response criteria are quantitative, reproducible, and simpler to apply, and have been widely used as surrogate endpoints in phase II trials. In this study, the media PFS of the responders was longer than that of the non-responders evaluated by each functional imaging parameter criteria and RECIST 1.1 criteria. Kaplan-Meier analysis results showed that the difference in PFS between the responders and non-responders evaluated by the RECIST 1.1 criteria were not statistically significant, whereas the differences were all statistically significant when evaluated by each functional imaging parameter criteria. Cox regression analysis results showed that ΔADC responders had a 64.9% reduction in risk compared to non-responders, and ΔD and %ΔD responders both had an 85.8% reduction in risk. In addition, results of the multivariate analysis of the association between PFS and each functional imaging parameter criteria demonstrated that the ADC and D evaluation response to therapy criteria were independent prognostic factors.

This study had several limitations. First, PFS was used as the major endpoint in tumor treatment. The Oncologic Drugs Advisory Committee recommended PFS as an endpoint for advanced NSCLC clinical trials in 2003 (22), but whether it can be used as a valid surrogate endpoint remains controversial (23,24). The lack of OS data is also a potential weakness, which it is hard to get though. Second, the study included a mixture of squamous cell carcinomas and adenocarcinomas, and the patient population was also very heterogeneous concerning the TNM classification. This is because the study cohort was too small to separate these groups. Third, in this study the chemotherapy regimen is not unified and not include Immune checkpoint inhibitor regimens which would be hope for non-responders. Further prospective analyses with a larger number of patients are warranted to confirm our findings. Finally, the MRI machines used were a mixture of 1.5T and 3.0T; the ROI was not drawn with 3D technique and volumetric-based histogram or texture ADC and DW-IVIM parameters maybe had higher reproducibility than did single-section (25); and the MRI parameter measurement was performed for one dominant lesion when multiple measurable lung lesions were present. These factors may have also affected the measured values of ADC and IVIM parameters.

Conclusions

The results of this study suggest that both D and ADC derived from diffusion-weighted MR imaging, rather than RECIST 1.1 criteria based on CT, are better at categorizing distinct responses and assessing the PFS of patients with NSCLC following anti-tumor therapy. Although ΔD was the best predictor of response to treatment, ΔADC measurement may simplify manual efforts and reduce the workload.

Acknowledgments

The authors appreciate the academic support from AME Lung Cancer Collaborative Group.
Funding: This work was supported by the National Natural Science Foundation of China (grant number 81571629, 82071990 and 81972187), Projects of the Committee of Shanghai Science and Technology (No. 19ZR1449800, 20Y11913700), Projects of the Shanghai Municipal Public Health Bureau (No. 201840122, 2019SY048), Doctoral Innovation Fund of Shanghai Jiao Tong University School of Medicine (No. BXJ201952), Interdisciplinary Program of Shanghai Jiao Tong University (No. YG2017MS80), and Project of Shanghai Talent Development Fund (No. 2019074).

Footnote

Reporting Checklist: The authors have completed the STARD reporting checklist. Available at https://dx.doi.org/10.21037/tlcr-21-610

Data Sharing Statement: Available at https://dx.doi.org/10.21037/tlcr-21-610

Conflicts of Interest: All authors have completed the ICMJE uniform disclosure form (available at https://dx.doi.org/10.21037/tlcr-21-610). The authors have no conflicts of interest to declare.

Ethical Statement: The authors are accountable for all aspects of the work in ensuring that questions related to the accuracy or integrity of any part of the work are appropriately investigated and resolved. All procedures performed in this study involving human participants were in accordance with the Declaration of Helsinki (as revised in 2013). The study was approved by ethics board of Shanghai Chest hospital, Shanghai Jiao Tong university (No.: ks1832) and informed consent was taken from all the patients.

References

1. Broncano J, Luna A, Sánchez-González J, et al. Functional MR Imaging in Chest Malignancies. Magn Reson Imaging Clin N Am 2016;24:135-55.
2. White NS, McDonald C, Farid N, et al. Diffusion-weighted imaging in cancer: physical foundations and applications of restriction spectrum imaging. Cancer Res 2014;74:4638-52.
3. Sumi M, Nakamura T. Head and neck tumors: assessment of perfusion-related parameters and diffusion coefficients based on the intravoxel incoherent motion model. AJNR Am J Neuroradiol 2013;34:410-6.
4. Du J, Li K, Zhang W, et al. Intravoxel Incoherent Motion MR Imaging: Comparison of Diffusion and Perfusion Characteristics for Differential Diagnosis of Soft Tissue Tumors. Medicine (Baltimore) 2015;94:e1028.
5. Deng Y, Li X, Lei Y, et al. Use of diffusion-weighted magnetic resonance imaging to distinguish between lung cancer and focal inflammatory lesions: a comparison of intravoxel incoherent motion derived parameters and apparent diffusion coefficient. Acta Radiol 2016;57:1310-7.
6. Qi LP, Yan WP, Chen KN, et al. Discrimination of Malignant versus Benign Mediastinal Lymph Nodes Using Diffusion MRI with an IVIM Model. Eur Radiol 2018;28:1301-9.
7. Zheng Y, Huang W, Zhang X, et al. A Noninvasive Assessment of Tumor Proliferation in Lung cancer Patients using Intravoxel Incoherent Motion Magnetic Resonance Imaging. J Cancer 2021;12:190-7.
8. Shi C, Liu D, Xiao Z, et al. Monitoring Tumor Response to Antivascular Therapy Using Non-Contrast Intravoxel Incoherent Motion Diffusion-Weighted MRI. Cancer Res 2017;77:3491-501.
9. Eisenhauer EA, Therasse P, Bogaerts J, et al. New response

evaluation criteria in solid tumours: revised RECIST guideline (version 1.1). Eur J Cancer 2009;45:228-47.
10. Reischauer C, Froehlich JM, Pless M, et al. Early treatment response in non-small cell lung cancer patients using diffusion-weighted imaging and functional diffusion maps--a feasibility study. PLoS One 2014;9:e108052.
11. Yabuuchi H, Hatakenaka M, Takayama K, et al. Non-small cell lung cancer: detection of early response to chemotherapy by using contrast-enhanced dynamic and diffusion-weighted MR imaging. Radiology 2011;261:598-604.
12. Yuan Z, Ye XD, Dong S, et al. Role of magnetic resonance diffusion-weighted imaging in evaluating response after chemoembolization of hepatocellular carcinoma. Eur J Radiol 2010;75:e9-14.
13. Vandecaveye V, Michielsen K, De Keyzer F, et al. Chemoembolization for hepatocellular carcinoma: 1-month response determined with apparent diffusion coefficient is an independent predictor of outcome. Radiology 2014;270:747-57.
14. Chen L, Zhang J, Chen Y, et al. Relationship between apparent diffusion coefficient and tumour cellularity in lung cancer. PLoS One 2014;9:e99865.
15. Le Bihan D, Breton E, Lallemand D, et al. Separation of diffusion and perfusion in intravoxel incoherent motion MR imaging. Radiology 1988;168:497-505.
16. Chenevert TL, McKeever PE, Ross BD. Monitoring early response of experimental brain tumors to therapy using diffusion magnetic resonance imaging. Clin Cancer Res 1997;3:1457-66.
17. Chenevert TL, Stegman LD, Taylor JM, et al. Diffusion magnetic resonance imaging: an early surrogate marker of therapeutic efficacy in brain tumors. J Natl Cancer Inst 2000;92:2029-36.
18. Lee EY, Yu X, Chu MM, et al. Perfusion and diffusion characteristics of cervical cancer based on intraxovel incoherent motion MR imaging-a pilot study. Eur Radiol 2014;24:1506-13.
19. Yan C, Xu J, Xiong W, et al. Use of intravoxel incoherent motion diffusion-weighted MR imaging for assessment of treatment response to invasive fungal infection in the lung. Eur Radiol 2017;27:212-21.
20. Wang LL, Lin J, Liu K, et al. Intravoxel incoherent motion diffusion-weighted MR imaging in differentiation of lung cancer from obstructive lung consolidation: comparison and correlation with pharmacokinetic analysis from dynamic contrast-enhanced MR imaging. Eur Radiol 2014;24:1914-22.
21. Liu X, Peng W, Zhou L, et al. Biexponential apparent diffusion coefficients values in the prostate: comparison among normal tissue, prostate cancer, benign prostatic hyperplasia and prostatitis. Korean J Radiol 2013;14:222-32.
22. McCain JA Jr. The ongoing evolution of endpoints in oncology. Manag Care 2010;19:1-11.
23. Soria JC, Massard C, Le Chevalier T. Should progression-free survival be the primary measure of efficacy for advanced NSCLC therapy? Ann Oncol 2010;21:2324-32.
24. Aggarwal C, Borghaei H. Treatment Paradigms for Advanced Non-Small Cell Lung Cancer at Academic Medical Centers: Involvement in Clinical Trial Endpoint Design. Oncologist 2017;22:700-8.
25. Yuan M, Zhong Y, Zhang YD, et al. Volumetric analysis of intravoxel incoherent motion imaging for assessment of solitary pulmonary lesions. Acta Radiol 2017;58:1448-56.

Cite this article as: Yuan Z, Niu XM, Liu XM, Fu HC, Xue TJ, Koo CW, Okuda K, Yao F, Ye XD. Use of diffusion-weighted magnetic resonance imaging (DW-MRI) to predict early response to anti-tumor therapy in advanced non-small cell lung cancer (NSCLC): a comparison of intravoxel incoherent motion-derived parameters and apparent diffusion coefficient. Transl Lung Cancer Res 2021;10(8):3671-3681. doi: 10.21037/tlcr-21-610

